THE GEOLOGICAL SOCIETY OF AMERICA®

Structural segmentation controlled the 2015 M_w 7.8 Gorkha earthquake rupture in Nepal

Judith Hubbard[1,2], Rafael Almeida[2], Anna Foster[2], Soma Nath Sapkota[3], Paula Bürgi[2], and Paul Tapponnier[2]
[1]Asian School of the Environment, Nanyang Technological University, Singapore 637459
[2]Earth Observatory of Singapore, Nanyang Technological University, Singapore 639798
[3]Department of Mines and Geology, Kathmandu 44600, Nepal

ABSTRACT

The ongoing collision of India with Asia is partly accommodated by slip on the Main Himalayan Thrust (MHT). The 25 April 2015, M_w 7.8 Gorkha earthquake is the most recent major event to rupture the MHT, which dips gently northward beneath central Nepal. Although the geology of the range has been studied for decades, fundamental aspects of its deep structure remain disputed. Here, we develop a structural cross section and a three-dimensional, geologically informed model of the MHT that are consistent with seismic observations from the Gorkha earthquake. A comparison of our model to a detailed slip inversion data set shows that the slip patch closely matches an oval-shaped, gently dipping fault surface bounded on all sides by steeper ramps. The Gorkha earthquake rupture seems to have been limited by the geometry of that fault segment. This is a significant step forward in understanding the deep geometry of the MHT and its effect on earthquake nucleation and propagation. Published models of fault locking do not correlate with the slip patch or our fault model in the vicinity of the earthquake, further suggesting that fault geometry was the primary control on this event. Our result emphasizes the importance of adequately constraining subsurface fault geometry in megathrusts in order to better assess the sizes and locations of future earthquakes.

INTRODUCTION

Many structural cross sections of the Himalaya have been developed over the past several decades, based on geology, topography, and seismicity (e.g., Le Fort, 1975; Stocklin, 1980; Schelling and Arita, 1991; Pandey et al., 1995; Pearson and DeCelles, 2005; Khanal and Robinson, 2013). They usually include an active thrust (Main Frontal Thrust [MFT]), exposed along the southern edge of the Sub-Himalayan foothills, which merges at depth with a fault (Main Himalayan Thrust [MHT]) that dips gently to the north beneath the Lesser Himalaya. This "décollement," or bed-parallel fault, in turn steepens downward onto a ramp that dives beneath the Higher Himalaya before flattening again northward under the Tethys Himalaya of southern Tibet. This ramp is necessary to produce the large Gorkha-Pokhara Anticlinorium (GPA), which extends through most of central Nepal, as well as the High Himalaya. Despite their overall similarity, the cross sections differ in significant features, such as the location, depth, and size of the ramp, the existence of other ramps, and the total amount of shortening. In addition, the sections drawn through the Kathmandu Klippe (Pearson and DeCelles, 2005; Khanal and Robinson, 2013) are not fully consistent with basic parameters of the Gorkha earthquake obtained from the global centroid-moment-tensor solution (GCMT; Ekström et al., 2012), such as the ~12 km depth and ~7° dip of the fault. These fault plane parameters are consistent with a joint slip inversion data set based on GPS, teleseismic, and interferometric synthetic aperture radar (InSAR) data, which indicate that the rupture extended ~140 km along strike and ~50 km downdip (Avouac et al., 2015). Such a rupture would be consistent with slip on a décollement.

STRUCTURAL CROSS SECTION

We present a cross section based on quantitative models of fault-related folding (assuming deformation by flexural slip and conservation of line length, thickness, and area; Suppe, 1983) that incorporates the regional geology (Stocklin, 1980; Geologic Map of Nepal [www.dmgnepal.gov.np/geology-of-nepal]; Pearson and DeCelles, 2005; Khanal and Robinson, 2013; Fig. DR1 in the GSA Data Repository[1]) and the fault orientation and depth from the main-shock GCMT solution. We propose that not one, but two active blind ramps bound the fault that slipped in the earthquake (Fig. 1). A deep, active, northern ramp is required to produce the GPA. A middle ramp to the south is required by the stratigraphy exposed in the hanging walls of the MFT and Main Boundary Thrust (MBT).

Both the MFT and MBT sole into the MHT. They are also both parallel to the rocks exposed in their hanging walls, which therefore reflect the stratigraphic levels to which they sole. However, these levels are different: The rocks above the MFT are mid-Miocene Lower Siwalik units, while those above the MBT are the Proterozoic Dandagaon Formation (Pearson and DeCelles, 2005; Khanal and Robinson, 2013). Based on this difference, we infer that the MBT, which formed first, rose from a deeper décollement within the Lesser Himalayan Sequence. When the fault system broke forward, it moved onto an upper décollement at the base of the Lower Siwalik units. This décollement truncated the frontal thrust, with the upper part of the MBT in its hanging wall. As slip continued south on faults in front of the MBT, the upper part of the MBT was progressively displaced, leaving the lower part behind as the middle ramp of the active fault.

We use this dual-ramp interpretation to build the cross section. Our section shows deformation postdating the largely ductile strain preserved in the Greater Himalayan Sequence (e.g., Le Fort, 1975). The earliest stage of deformation (Figs. 1A and 1B) occurs on the thrust termed the Ramgarh Thrust (Pearson and DeCelles, 2005) or brittle Main Central Thrust (MCT; Searle et al., 2008), which underlies the greenschist-facies rocks at the base of the Greater Himalayan Sequence. The distinction affects pre–13 Ma shortening estimates, but it does not change our structural cross section. We refer to this fault as the MCT herein.

In a second stage (Figs. 1B and 1C), a new, deeper décollement level developed, and a new ramp broke forward within the rocks of the Lesser Himalayan Sequence; this geometry is necessary in the reconstruction because the original MCT décollement is now refolded, eroded, and exposed both continuously at the base of the High Himalaya, and as klippen to the south.

A third stage of deep ramp formation (Figs. 1D and 1E) is required to have produced the steep dips (up to 70°; Fig. DR1) on either side of the

[1]GSA Data Repository item 2016206, triangulated surface of MHT fault model in xyz format, and Figures DR1–DR6 (cross section from Figure 1F showing exaggerated topography, and map views of Main Himalayan Thrust), is available online at www.geosociety.org/pubs/ft2016.htm, or on request from editing@geosociety.org.

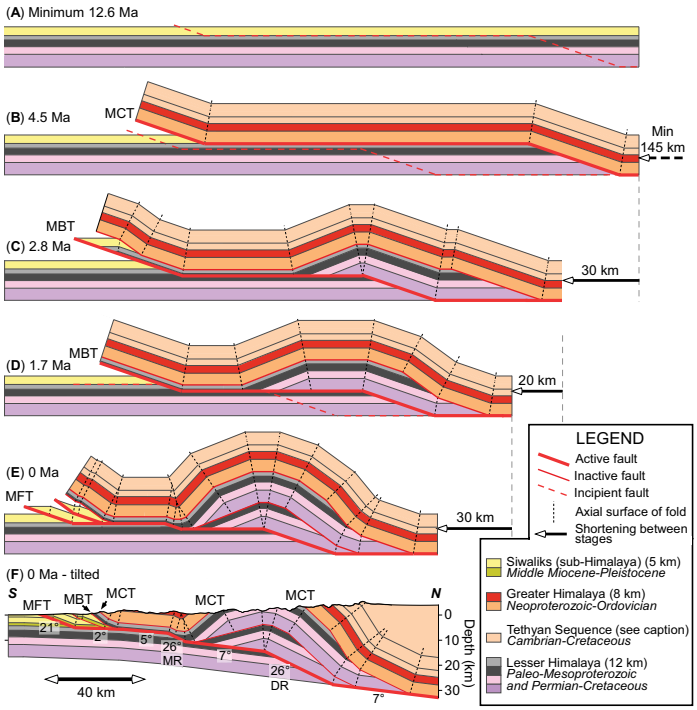

Figure 1. Progressive structural development in central Nepal. A–E: Deformation assuming horizontal, uniform-thickness stratigraphy. F: Adjusted to flexure of Indian plate, with units above Main Central Thrust (MCT) colored to match mapped geology. Name, age, and thickness of each unit are shown in legend. Tethyan Sedimentary Sequence and underlying rocks are internally deformed; represented thickness is not stratigraphic. Shortening at each stage is indicated on right, and resulting age (minimum) is estimated by assuming that modern shortening rate of 17.8 mm/yr (Ader et al., 2012) has been constant since the Miocene. A: Undeformed. B: MCT active; Greater Himalayan and Tethyan rocks originate north (right) of A. C–D: Main Boundary Thrust (MBT) active, with development of new deep ramp. E: Main Frontal Thrust (MFT) and other Siwalik faults active, with development of final deep ramp (DR) under the Gorkha-Pokhara Anticlinorium (GPA). Note that between D and E, base of the MBT is offset from its top, leaving behind an active middle ramp (MR). F: Dip of each section of Main Himalayan Thrust (MHT) model is noted underneath the fault, and beds and faults above are tilted accordingly.

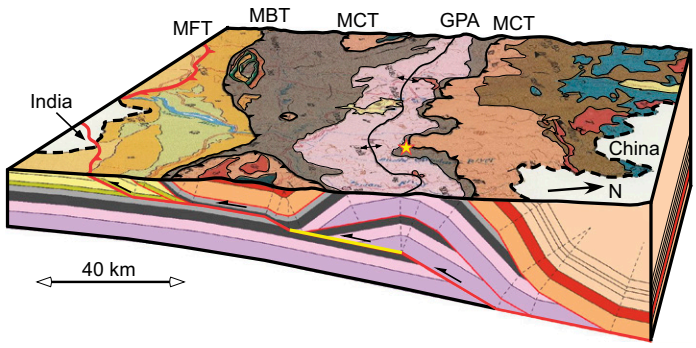

Figure 2. Block model of Nepal Himalaya, showing agreement of cross section (Fig. 1F) with surface geology (Geologic Map of Nepal [www.dmgnepal.gov.np/geology-of-nepal]). Yellow portion of Main Himalayan Thrust (MHT) corresponds to main-shock rupture patch of Gorkha earthquake. Yellow star shows surface projection of rupture initiation point (Avouac et al., 2015). Unit colors are same as in Figure 1. MCT—Main Central Thrust; MBT—Main Boundary Thrust; MFT—Main Frontal Thrust; GPA—Gorkha-Pokhara Anticlinorium.

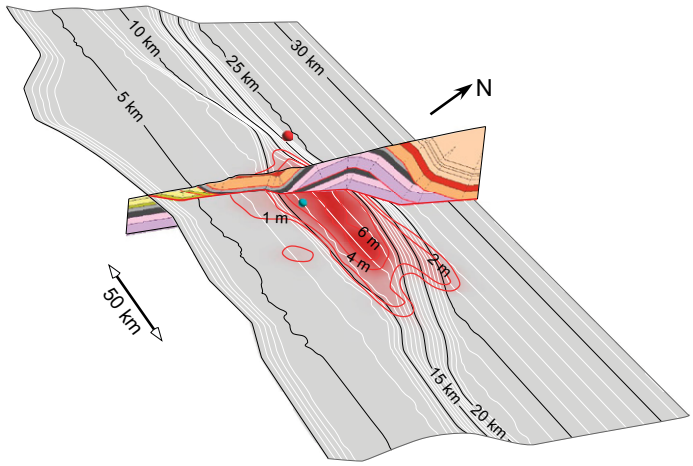

Figure 3. Perspective view of Main Himalayan Thrust. Black and white contours show depth below sea level to thrust surface. Red area and contours show slip amounts during Gorkha earthquake; red dot is hypocenter location (Avouac et al., 2015). Blue dot is Kathmandu. Cross section is same as Figure 1F.

GPA through refolding, and to raise the rocks in the hinge of the GPA enough to be exposed at the surface. The development of the upper décollement level at this stage resulted in the formation of the middle ramp.

Currently (Fig. 1F), the active deep ramp to the north represents the latest and deepest of a series of three deep ramps that have broken forward over time, producing a refolded, or imbricated duplex. The middle and upper décollements are connected by the active middle ramp. The topographic signature of the middle ramp can be seen north of the Kathmandu Valley, where the Sheopuri Lekh range stands ~1200 m above the valley floor (Fig. DR2). The final section is consistent with the exposed geology (Fig. 2).

THREE-DIMENSIONAL FAULT MODEL

We extended the cross section laterally to create a three-dimensional (3-D) structural model using Gocad (Mallet, 1992; Fig. 3), making three constraints/assumptions based on the previous discussion:

(1) The MFT is located at the topographic break at the front of the system (Fig. DR3).

(2) The middle ramp can be traced along strike using the MBT as a proxy (Fig. DR3), because in our model, the distance between the top of the middle ramp and the base of the MBT is determined by the total slip on all faults south of the MBT. We used a value of 21 km for this distance. This amount is within the range of shortening estimates for central and eastern Nepal found by previous authors (15–40 km; Schelling and Arita, 1991; Schelling et al., 1991; Mugnier et al., 1999; Hirschmiller et al., 2014). This range is in part due to differences in balancing methods and depth to décollement used in different studies. However, when the same techniques and assumptions are used, the shortening amount does not vary significantly along strike, at least in central Nepal (Hirschmiller et al., 2014), suggesting that while the total amount is not well constrained, the slip past the MBT remains relatively constant along strike. This allows us to use the MBT as a proxy for the shape of the middle ramp.

(3) The top of the deep ramp can be traced along strike using the axis of the GPA as a proxy (Fig. DR3).

The resulting regional MHT model is shown in Figures 3 and 4 and in Figure DR4. A digital file with the fault geometry for all of Nepal is available in the Data Repository. Within the region of the Gorkha earthquake, the two ramps are separated by a middle décollement. However, to the east and west, the ramps approach each other, merging to yield a single large ramp with no middle décollement; we call these junctions

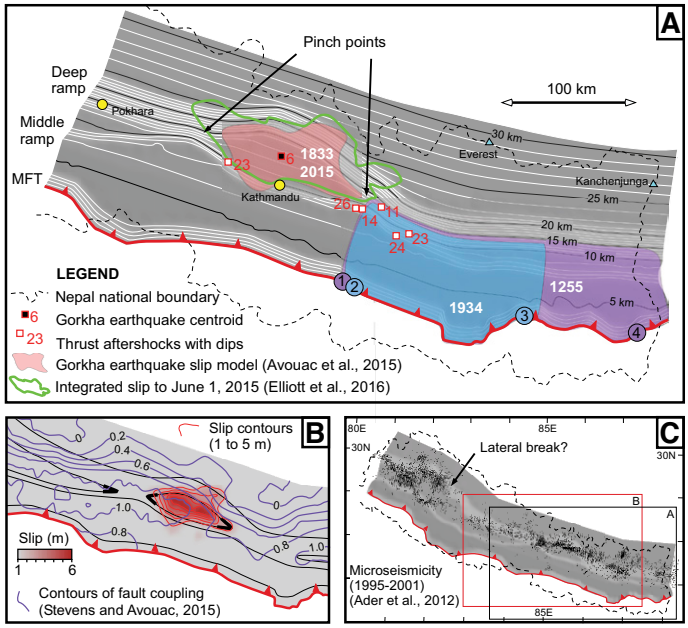

Figure 4. A: Map view of Main Himalayan Thrust (MHT) in central and eastern Nepal. Contours show depth to thrust surface. Possible slip patches for historical earthquakes are outlined; areas measured from fault model are (in 1000 km²): 3.5 (A.D. 2015, 1833), 10.1 (1934), and 16.3 (1255). Purple and blue circles are trenching sites identifying A.D. 1255 and 1934 ruptures (1—Lavé et al., 2005; 2—Sapkota et al., 2012; 3—P. Tapponnier, 2016, personal commun.; 4—Nakata et al., 1998). MFT—Main Frontal Thrust. B: Comparison of fault geometry with slip model from A and with fault coupling on MHT for area around Gorkha earthquake. Geometric pinch points are highlighted in bold. C: Fault model for all of Nepal with microseismicity. Locations of A and B are marked in C. Larger versions of fault model with fault traces, coupling model, and microseismicity are provided in Data Repository (see text footnote 1).

"pinch points" (bold lines in Fig. 4B), as the middle décollement pinches out. This model geometry is the consequence of the curvature of the MBT and the GPA. Toward western Nepal, the MBT and GPA, and hence the middle ramp and deep ramp, diverge once more, and the middle décollement is again present.

COMPARISON OF THE FAULT MODEL WITH EARTHQUAKE SLIP AND SEISMICITY

Strikingly, when we compare our fault model to the Gorkha earthquake coseismic slip inversion data set (updated version of Avouac et al. [2015] model; Wei, 2016, personal commun.), we see that the location and shape of slip (>1 m) match closely with the location and shape of an isolated patch of middle décollement bounded on all sides by ramps (Fig. 3). This indicates that not only is the main active fault composed of several discrete segments with different dips, but that this geometry controlled the shape and size of the main-shock rupture. Thus, subsurface fault geometry may play an important part in defining rupture patches elsewhere. Beyond the Gorkha rupture zone, we observe no other pinch points in the Nepal Himalaya—the middle décollement extends for over 400 km westward, while the single larger ramp (middle ramp + deep ramp) dominates to the east (Fig. 4). In far western Nepal, the deep ramp has an abrupt shift to the north. We propose that this may be a lateral break in the MHT that may act as a barrier to slip in some earthquakes.

A comparison of our model to relocated earthquakes ($M_w \geq 2$) from A.D. 1995 to 2001 (Ader et al., 2012) shows that the lateral break matches a change in the distribution of microseismicity (Fig. 4C; Fig. DR5), which has been suggested to be associated with a change from a single ramp to an active duplex structure (Harvey et al., 2015). In eastern Nepal, the microseismicity, commonly associated with the deep ramp, outlines the northeastern edge of the slip patch.

GCMT focal mechanisms are available for six thrust-mechanism aftershocks following the Gorkha earthquake (M_w 5.1–7.3; Fig. 4A). If we assume that these aftershocks occurred on the MHT, then we can compare the nodal plane dips with the local dip of our modeled MHT. The north-dipping nodal planes of four of the aftershocks dip 23°–26° and line up along the middle ramp, and a fifth, located close to the eastern pinch point, dips 14°, all of which are consistent with our model. The largest aftershock (M_w 7.3) is ambiguous: Reported depths range from 12 km to 28 km (National Earthquake Information Center, 2015). This earthquake could have occurred on the deep décollement or on an unidentified fault in its hanging wall.

LONG-TERM CONTROL OF FAULT GEOMETRY ON SEISMICITY

Geodetic studies have shown that the MHT is locked, and they have constrained the downdip extent of coupling (Ader et al., 2012; Stevens and Avouac, 2015). When we compare the downdip transition zone of these coupling models to our fault geometry, we note that it follows our deep ramp in western Nepal, but not in the Gorkha earthquake region (Fig. 4B; Fig. DR6). It seems that although the coupling pattern is largely a consequence of fault depth and geometry, it is also complicated by other factors. Within the coupling transition zone, we expect to see a combination of coseismic and interseismic slip. A comparison of the coseismic slip model of Avouac et al. (2015) and the slip model of Elliott et al. (2016), which includes deformation up to 1 June 2015, shows that both have similar updip boundaries, but the longer-period observation includes significantly more slip on the deep ramp (Fig. 4A). The key observation is that neither the coupling nor any previously proposed fault geometries (e.g., Elliott et al., 2016) can explain the shape and abrupt gradients in slip observed in the Gorkha earthquake, whereas the changes in fault geometry can.

The active fault geometry varies at the time scale of millions of years (Figs. 1A–1D); however, the geometric barriers should have remained roughly constant for the last million years (Figs. 1D and 1E). The paleoseismological record is limited, but the last earthquake that occurred in the region (1833) seems to have been controlled by the fault geometry. The rupture area and size (M_w 7.5–7.9) of the A.D. 1833 earthquake have been estimated using intensity reports (Bilham, 1995; Szeliga et al., 2010) and closely resemble those of the Gorkha earthquake.

On the upper décollement, neither coseismic nor measurable afterslip occurred following the Gorkha earthquake (Grandin et al., 2015; Lindsey et al., 2015; Elliott et al., 2016), leaving open the question of how convergence is accommodated on this part of the fault. Studies suggest that in very large historical events, the MHT ruptured coseismically to the surface (e.g., A.D. 1255, 1505, 1934; Nakata et al., 1998; Sapkota et al., 2012; Bollinger et al., 2014), and that the majority of Himalayan convergence reaches the frontal fault as slip (Lavé and Avouac, 2000). Thus, we expect that the upper décollement will produce large slip events. Great earthquakes likely initiate at the base of the seismogenic zone and rupture through geometric barriers to the surface. Smaller earthquakes, however, seem to break geometry-controlled patches, and some of these may be limited to the upper décollement.

Empirical relationships can be used to estimate earthquake magnitude based on slip area (Hanks and Bakun, 2008). The magnitudes empirically inferred for both the Gorkha and the 1934 earthquakes based on their reported slip areas match their instrumentally inferred magnitudes (M_w 7.8 and M_w 8.4, respectively; Chen and Molnar, 1977; Sapkota et al., 2012; Avouac et al., 2015). This suggests that this method is appropriate, so we used it to examine the areas of discrete fault segments in our model. The area of the upper décollement south of the Gorkha earthquake (Fig. 4A) would correspond to M_w 8.0, much larger than any known earthquake there.

West of the Gorkha region, the fault area consisting of both the middle and upper décollements could produce an earthquake up to M_w 9.2, although

the middle ramp and potential lateral break could serve as geometric rupture barriers, limiting earthquake size. Scarce historical records are not sufficient to constrain possible scenarios. In eastern Nepal, trenching studies have defined the extent of surface rupture for the 1255 and 1934 earthquakes (Fig. 4A; Nakata et al., 1998; Sapkota et al., 2012; Bollinger et al., 2014). Based on the reported extent of the 1255 earthquake, we can infer a magnitude up to M_w 8.7 for this event. In our fault model, there are no geometric barriers or pinch points in this region that could have limited earthquake rupture. The difference in lateral extent of the 1255 and 1934 earthquakes is a reminder that other types of slip barriers also limit rupture areas.

CONCLUSIONS

We produced a new cross section of the central Nepal Himalaya, using constraints from surface geology and the 2015 Gorkha earthquake. Our section requires a middle ramp, separating a middle and upper décollement, in addition to the deep ramp traditionally understood to be responsible for the growth of the Gorkha-Pokhara Anticlinorium. We extended the cross section into a 3-D model of the MHT for all of Nepal using surface geology. By comparing our model with an independent slip inversion data set, we show that variations in fault orientation at depth were likely responsible for limiting the size of the Gorkha earthquake.

Geometric boundaries such as bends and step-overs in map view have been interpreted to act as persistent barriers to rupture on strike-slip faults (Wesnousky, 2006), but for thrust faults, the role of subsurface geometry is less well known (King and Nabelek, 1985). For these faults, characteristics such as changes in fault zone properties or footwall or hanging-wall structure are thought to control the distribution and size of ruptures. Our results suggest that geometric changes are equally important in collision megathrusts. Detailed studies of the geometries of these convergent systems should therefore help better assess seismic hazard by identifying constraints on the sizes and locations of future earthquakes.

ACKNOWLEDGMENTS

We thank the editor and the reviewers (Jean-Philippe Avouac, Richard Briggs, and two anonymous reviewers) for their thoughtful comments and suggestions, which helped us to improve the manuscript. This research was supported by the National Research Foundation (NRF) Singapore under its NRF Fellowship scheme (award no. NRF-NRFF2013–06) and by the EOS and the NRF Singapore and the Singapore Ministry of Education under the Research Centres of Excellence initiative. This work comprises Earth Observatory of Singapore (EOS) contribution 106.

REFERENCES CITED

Ader, T., et al., 2012, Convergence rate across the Nepal Himalaya and interseismic coupling on the Main Himalayan Thrust: Implications for seismic hazard: Journal of Geophysical Research, v. 117, p. B04403, doi:10.1029/2011JB009071.

Avouac, J.P., Meng, L., Wei, S., Wang, T., and Ampuero, J.P., 2015, Lower edge of locked Main Himalayan Thrust unzipped by the 2015 Gorkha earthquake: Nature Geoscience, v. 8, p. 708–711, doi:10.1038/ngeo2518.

Bilham, R., 1995, Location and magnitude of the 1833 Nepal earthquake and its relation to the rupture zones of contiguous Great Himalayan earthquakes: Current Science, v. 69, p. 101–128.

Bollinger, L., Sapkota, S.N., Tapponnier, P., Klinger, Y., Rizza, M., Van der Woerd, J., Tiwari, D.R., Pandey, R., Bitri, A., and Bes de Berc, S., 2014, Estimating the return times of great Himalayan earthquakes in eastern Nepal: Evidence from the Patu and Bardibas strands of the Main Frontal Thrust: Journal of Geophysical Research, v. 119, p. 7123–7163, doi:10.1002/2014JB010970.

Chen, W.-P., and Molnar, P., 1977, Seismic moments of major earthquakes and the average rate of slip in Central Asia: Journal of Geophysical Research, v. 82, p. 2945–2969, doi:10.1029/JB082i020p02945.

Ekström, G., Nettles, M., and Dziewonski, A.M., 2012, The global CMT project 2004–2010: Centroid-moment tensors for 13,017 earthquakes: Physics of the Earth and Planetary Interiors, v. 200–201, p. 1–9, doi:10.1016/j.pepi.2012.04.002.

Elliott, J.R., Jolivet, R., González, P.J., Avouac, J.-P., Hollingsworth, J., Searle, M.P., and Stevens, V.L. 2016, Himalayan megathrust geometry and relation to topography revealed by the Gorkha earthquake: Nature Geoscience, v. 9, p. 174–180, doi:10.1038/ngeo2623.

Grandin, R., Vallée, M., Satriano, C., Lacassin, R., Klinger, Y., Simoes, M., and Bollinger, L., 2015, Rupture process of the Mw = 7.9 2015 Gorkha earthquake (Nepal): Insights into Himalayan megathrust segmentation: Geophysical Research Letters, v. 42, p. 8373–8382, doi:10.1002/2015GL066044.

Hanks, T., and Bakun, W.H., 2008, M-log A observations for recent large earthquakes: Bulletin of the Seismological Society of America, v. 98, p. 490–494, doi:10.1785/0120070174.

Harvey, J.E., Burbank, D.W., and Bookhagen, B., 2015, Along-strike changes in Himalayan thrust geometry: Topographic and tectonic discontinuities in western Nepal: Lithosphere (in press), doi:10.1130/L444.1.

Hirschmiller, J., Grujic, D., Bookhagen, B., Coutand, I., Huyghe, P., Mugnier, J.-L., and Ojha, T., 2014, What controls the growth of the Himalayan foreland fold-and-thrust belt?: Geology, v. 42, p. 247–250, doi:10.1130/G35057.1.

Khanal, S., and Robinson, D., 2013, Upper crustal shortening and forward modeling of the Himalayan thrust belt along the Budhi-Gandaki River, central Nepal: International Journal of Earth Sciences, v. 102, p. 1871–1891, doi:10.1007/s00531-013-0889-1.

King, G.C.P., and Nabelek, J., 1985, Role of fault bends in the initiation and termination of earthquake rupture: Science, v. 228, p. 984–987, doi:10.1126/science.228.4702.984.

Lavé, J., and Avouac, J.P., 2000, Active folding of fluvial terraces across the Siwaliks Hills, Himalayas of central Nepal: Journal of Geophysical Research, v. 105, p. 5735–5770, doi:10.1029/1999JB900292.

Le Fort, P., 1975, Himalaya: The collided range: Present knowledge of the continental arc: American Journal of Science, v. 275A, p. 1–44.

Lindsey, E.O., Natsuaki, R., Xu, X., Shimada, M., Hashimoto, M., Melgar, D., and Sandwell, D., 2015, Line of sight displacement from ALOS-2 interferometry: M7.8 Gorkha earthquake and Mw 7.3 aftershock: Geophysical Research Letters, v. 42, p. 6655–6661, doi:10.1002/2015GL065385.

Mallet, J.L., 1992, Discrete smooth interpolation in geometric modeling: Computer Aided Design, v. 24, p. 178–191, doi:10.1016/0010-4485(92)90054-E.

Mugnier, J., Leturmy, P., Huyghe, P., Chalaron, E., Vidal, G., Husson, L., and Delcaillau, B., 1999, The Siwaliks of western Nepal: I. Geometry and kinematics: Journal of Asian Earth Sciences, v. 17, p. 629–642, doi:10.1016/S1367-9120(99)00038-3.

Nakata, T., Kumura, K., and Rockwell, T., 1998, First successful paleoseismic trench study on active faults in the Himalaya: Eos, Transactions, American Geophysical Union, v. 79, p. F615.

National Earthquake Information Center, 2015, Moment Tensor Page for 25 April 2015 Nepal Earthquake: http://earthquake.usgs.gov/earthquakes/eventpage/us20002ejl#scientific_tensor (June 2016).

Pandey, M., Tankudar, R., Avouac, J.P., Lavé, J., and Massot, J.P., 1995, Interseismic strain accumulation on the Himalayan crustal ramp (Nepal): Geophysical Research Letters, v. 22, p. 751–754, doi:10.1029/94GL02971.

Pearson, O.N., and DeCelles, P.G., 2005, Structural geology and regional tectonic significance of the Ramgarh thrust, Himalayan fold-thrust belt of Nepal: Tectonics, v. 24, p. TC4008, doi:10.1029/2003TC001617.

Sapkota, S.N., Bollinger, L., Klinger, Y., Tapponnier, P., Gaudemer, Y., and Tiwari, D., 2012, Primary surface rupture of the great Himalayan earthquakes of 1934 and 1255: Nature Geoscience, v. 6, p. 71–76.

Schelling, D., and Arita, K., 1991, Thrust tectonics, crustal shortening and the structure of the far-eastern Nepal Himalaya: Tectonics, v. 10, p. 851–862, doi:10.1029/91TC01011.

Schelling, D., Cater, J., Seago, R., and Ojha, T.P., 1991, A balanced cross-section across the central Nepal Siwalik Hills; Hitauda to Amlekhganj: Journal of the Faculty of Science: Hokkaido University, v. 23, p. 1–9.

Searle, M., Law, R., Godin, L., Larson, K., Streule, M., Cottle, J., and Jessup, M., 2008, Defining the Himalayan Main Central Thrust in Nepal: Journal of the Geological Society of London, v. 165, p. 523–534, doi:10.1144/0016-76492007-081.

Stevens, V.L., and Avouac, J.-P., 2015, Interseismic coupling on the main Himalayan thrust: Geophysical Research Letters, v. 42, p. 5828–5837, doi:10.1002/2015GL064845.

Stocklin, J., 1980, Geology of Nepal and its regional frame: Journal of the Geological Society of London, v. 137, p. 1–34, doi:10.1144/gsjgs.137.1.0001.

Suppe, J., 1983, Geometry and kinematics of fault-bend folding: American Journal of Science, v. 283, p. 684–721, doi:10.2475/ajs.283.7.684.

Szeliga, W., Hough, S., Martin, S., and Bilham, R., 2010, Intensity, magnitude, location, and attenuation in India for felt earthquakes since 1762: Bulletin of the Seismological Society of America, v. 100, p. 570–584, doi:10.1785/0120080329.

Wesnousky, S.G., 2006, Predicting the endpoints of earthquake ruptures: Nature, v. 444, p. 358–360, doi:10.1038/nature05275.

Manuscript received 9 May 2016
Revised manuscript received 9 June 2016
Manuscript accepted 16 June 2016

Printed in USA